

# **An experimental chemical kinetic study of the oxidation of diethyl ether in a jet-stirred reactor and comprehensive modeling**

Zeynep Serinyel<sup>1,2\*</sup>, Maxence Lailliau<sup>1,2</sup>, Sébastien Thion<sup>1,2†</sup>, Guillaume Dayma<sup>1,2</sup>, Philippe Dagaut<sup>1</sup>

<sup>1</sup> CNRS-INSIS, Institut de Combustion, Aérothermique, Réactivité et Environnement 1C, Avenue de la recherche scientifique, 45071 Orléans cedex 2, France

<sup>2</sup> Université d'Orléans, 6 Avenue du Parc Floral, 45100 Orléans, France

## **Full-length article**

### **Corresponding author:**

Zeynep Serinyel, PhD  
Institut de Combustion Aérothermique Réactivité et Environnement  
Université d'Orléans  
1C avenue de la Recherche Scientifique  
45071 Orléans cedex 2  
FRANCE  
Tel : +33 2 38 25 77 77  
e-mail : [zeynep.serinyel@cnrs-orleans.fr](mailto:zeynep.serinyel@cnrs-orleans.fr)

Keywords: Jet-stirred reactor, diethyl ether, oxidation, chemical kinetics

† Present address : Electricité de France (EDF), 6 Quai Watier, 78400 Chatou, France

sebastien.thion@edf.fr

# **An experimental chemical kinetic study of the oxidation of diethyl ether in a jet-stirred reactor and comprehensive modeling**

Zeynep Serinyel<sup>1,2†</sup>, Maxence Lailliau<sup>1,2</sup>, Sébastien Thion<sup>1,2</sup>, Guillaume Dayma<sup>1,2</sup>, Philippe Dagaut<sup>1</sup>

<sup>1</sup> CNRS-INSIS, Institut de Combustion, Aérodynamique, Réactivité et Environnement 1C, Avenue de la recherche scientifique, 45071 Orléans cedex 2, France

<sup>2</sup> Université d'Orléans, 6 Avenue du Parc Floral, 45100 Orléans, France

†Corresponding author: zeynep.serinyel@cnrs-orleans.fr

## **Abstract**

The oxidation of diethyl ether was studied experimentally in a jet-stirred reactor. Fuel-lean, stoichiometric and fuel-rich mixtures were oxidized at a constant fuel mole fraction (1000 ppm), at temperatures ranging from 450 to 1250 K, pressures of 1 and 10 atm, and constant residence time (70 and 700 ms, respectively). In total, six mixtures were tested at both pressures. Mole fraction profiles were obtained using gas chromatography and Fourier transform infrared spectrometry. The fuel mole fraction profiles, as well as some reaction intermediate and product profiles indicated strong low-temperature chemistry at high pressure. On the other hand, at atmospheric pressure this behavior was observed to a very small extent and only with the lean and stoichiometric mixture. These data were compared to modeling results using literature mechanisms for diethyl ether oxidation. None of these predicted low-temperature reactivity under present conditions. Therefore, a kinetic mechanism is proposed in this study, based on recently computed kinetic parameters from literature. It shows good performances for representing the present experimental data as well as experimental data found in literature consisting of ignition delay times, laminar flame speeds and flame structure.

## Introduction

Given the strict emission regulations for automotive sector and environmental concerns, there has recently been a growing need to find alternative feedstocks for the next generation biofuels. Diethyl ether (DEE) could represent an alternative fuel for compression ignition engines given its high cetane number ( $> 125$ ) and because it can be produced from bio-ethanol by dehydration.

Previous combustion related studies on diethyl ether include structure and burning velocity of laminar flames [1-3], ignition delay times [4] and pyrolysis/oxidation in a shock tube and jet-stirred reactor [5, 6]. To the best of our knowledge, the earliest speciation study on DEE was reported in the 60's by Agnew and Agnew [7] in a stabilized flat flame for rich DEE/air mixtures at atmospheric pressure. They identified and quantified an important number of species among which the cyclic ether 2-methyl-1,3-dioxolane. Yasunaga et al. [6] studied pyrolysis and oxidation of diethyl ether behind reflected shock waves, above 900 K. Tran and co-workers [2] reported species profiles in a rich premixed low-pressure flame as well as laminar burning velocities of DEE in a constant volume cylindrical chamber between 1–5 atm, and they have also studied the effect of blending DEE to n-butane flames and showed a decrease in soot precursor formation compared to a neat n-butane flame [3]. Vin et al. [5] studied pyrolysis of DEE in a jet-stirred reactor between 200–800 Torr and 600–1100 K. They observed complete destruction of the reactant at 1080 K for a residence time of 2 s and reported CO, methane, ethylene and acetaldehyde as major products. Werler and co-workers [4] measured ignition delay times of DEE in a shock tube (900–1300 K) and a rapid compression machine (500–1060 K) at high pressure. They observed two-stage ignition in RCM experiments. Laminar flame speed of DEE has also been studied by several groups [1, 8, 9]. There has been some recent theoretical investigations on the low-temperature chemistry

of DEE by Sakai and co-workers [10, 11], who computed thermochemistry and rate constants of the related species and reactions, and proposed a kinetic reaction mechanism.

This study investigates the oxidation of DEE in a jet-stirred reactor spanning an interval from low- to high-temperatures showing cool flame and negative temperature coefficient (NTC) behavior for all mixtures ( $\phi = 0.5, 1, 2$ ) at 10 atm. The experimental conditions chosen in this study are the same as in our dibutyl ether (DBE) experiments, previously reported [12]. Unlike the unconventional “double-NTC” behavior observed in DBE, DEE shows a conventional but very strong cool flame and NTC behavior, a comparison will be presented in coming sections.

## **1. Jet-stirred reactor experiments**

Experiments were carried out in a fused silica jet-stirred reactor settled inside a stainless-steel pressure resistant jacket. An electrical oven enabled to perform experiments up to c.a. 1280K. The temperature within the reactor was continuously monitored by a Pt/Pt-Rh thermocouple located inside a thin wall fused silica tube to prevent catalytic reactions on the metallic wires. Initial fuel mole fraction was 1000 ppm for all experiments, pressure and residence time ( $\tau$ ) were held constant at 1 and 0.07s or 10 atm and 0.7s. The reactive mixtures were highly diluted by nitrogen to avoid high heat release inside the reactor and experiments were performed at temperatures ranging from 450 to 1280 K as in our previous work [12]. The liquid fuel was atomized by a nitrogen flow and vaporized through a heated chamber. Reactants were brought separately to the reactor to avoid premature reactions and then injected by 4 injectors providing stirring. Flow rates of the diluent and reactants were controlled by mass flowmeters. A low-pressure sonic probe was used to freeze the reactions and take samples of the reacting mixtures.

As previously [12], online analyses were performed after sending the samples via a heated line to a Fourier transform infrared (FTIR) spectrometer for the quantification of H<sub>2</sub>O, CO, CO<sub>2</sub>, and CH<sub>2</sub>O. Samples were also stored at ca. 40 mbar in Pyrex bulbs for further analyses using gas chromatography (GC). Two gas chromatographs with a flame ionization detector (FID) were used: one equipped with a DB624 column to quantify oxygenated compounds and the other one with a CP-Al<sub>2</sub>O<sub>3</sub>/KCl column to quantify hydrocarbons. Identification of the products was done by GC/MS on a Shimadzu GC2010 Plus, with electron impact (70 eV) as the ionization mode. Hydrogen profiles were measured using a GC-TCD equipped with a CP-CarboPLOT P7 column. The species quantified in this study include diethyl-ether (DEE), H<sub>2</sub>, H<sub>2</sub>O, CO, CO<sub>2</sub>, C<sub>2</sub>H<sub>4</sub>, CH<sub>4</sub>, C<sub>2</sub>H<sub>6</sub>, C<sub>3</sub>H<sub>6</sub>, formaldehyde, acetic acid, acetaldehyde, 2-methyl-1,3-dioxolane and traces of ethoxy ethene (less than 2 ppm). The carbon balance was checked for each sample and was found to be within  $\pm 10\%$ .

## 2. Kinetic mechanism

A kinetic sub-mechanism representing low- and high-temperature chemistry of DEE is proposed in this study as none of the literature models could represent the experimental behavior (cool flame and NTC) observed. Fuel mole fraction profile at 10 atm for the lean mixture is presented in the supplementary material, figure S1, for this matter. The base mechanism is the DBE mechanism previously reported [12] and a sub-mechanism of DEE was introduced within. In the present DEE sub-mechanism, rate constants of the main reactions were adopted from the literature, main features are as follows:

- Reactions of hydrogen abstraction from fuel by H atoms and OH radicals are taken analogous to ethanol system proposed by Sivaramakrisnan et al. [13] for the primary site. For the C–H bond adjacent to the ether function, the rate constants are adopted

from Zhou et al. [14] for H-abstraction by OH radicals, and from Ogura et al. [15] for H-abstraction by H atoms.

- H-abstraction rate constants by HO<sub>2</sub> and CH<sub>3</sub> radicals are adopted from the theoretical studies of Mendes et al. [16] and Xu et al. [17], respectively.
- Rate constants adopted from Goldsmith et al. [18] for R+O<sub>2</sub> ⇌ RO<sub>2</sub> reactions, both for 1<sup>st</sup> and 2<sup>nd</sup> addition.
- Rate constants adopted from Villano et al. [19, 20] for RO<sub>2</sub> ⇌ QOOH, QOOH ⇌ cyclic ether + OH.
- Beta-scission reactions of fuel radicals and those of QOOH radicals are adopted from the CBS-QB3 calculations of Sakai et al. [11], and from our previous calculations on DBE [12]. Among the latter reactions, only the decomposition of the QOOH radical resulting from the isomerization of the secondary RO<sub>2</sub> appears to be of importance influencing the extent of the NTC, as will be explained in the coming sections.
- Other reactions related to low-temperature chemistry are taken analogous to our previous DBE study [12].
- Unimolecular decomposition reactions of DEE were taken from the study of Yasunaga et al. [6].

Thermochemistry of the fuel, fuel radical as well as all related low-temperature species were taken from the theoretical study of Sakai et al. [11], and for other species these were calculated using Thergas [21] which uses group additivity methods as proposed by Benson [22]. Kinetic mechanism and thermochemistry files can be found in the supplementary material. Simulations were carried out with the Chemkin II package. The Perfectly Stirred Reactor (PSR) code [23] was used to perform simulations for the JSR. For ignition delays Senkin [24], and for flame speed and structure calculations Premix [25] were used. Results are shown in the following figures.

### 3. Results and discussion

Experimental and model evolution of fuel consumption for all sets of experiments are presented in Figure 1. At atmospheric pressure, the  $\phi = 2$  mixture shows no reactivity up to around 950 K while the lean mixture shows some reactivity between 500–600K (~20% conversion at 570 K) and the  $\phi = 1$  mixture as well but to a much lower extent. According to the model, high temperature reactivity begins around 950 K, at all equivalence ratios in agreement with the data. The kinetic model also captures the low-temperature reactivity, slightly over-predicting it at maximum fuel conversion. On the other hand, at 10 atm, reactivity kicks off at very low temperatures (10% fuel conversion at 480 K,  $\phi = 0.5$ ) and reaches its maximum around 510 K. Such high reactivity was also observed previously with dibutyl ether oxidation [12] performed under similar experimental conditions. Although fuel reactivity goes back to zero around 700 K for the  $\phi = 2$  mixture, 7% fuel conversion is observed at 750 K for the  $\phi = 0.5$  mixture. These behaviors are correctly captured by the kinetic model, except for the extent of the NTC region of the lean mixture which is under-predicted. Also, one should note that the cool flame / NTC is observed for a larger temperature interval for the lean mixture (510–750 K) compared to the rich mixture (510–700 K). Furthermore, it was observed that, as opposed to 10 atm experiments, ethanol is quantified at 1 atm. This is a product of the unimolecular decomposition of DEE into ethanol and ethylene. The corresponding rate parameters were adopted from Yasunaga mechanism [6].

#### *10 atm experiments*

Figures 2–4 show the evolution of intermediate species and reaction products as a function of the reactor temperature at 10 atm. Owing to its symmetric structure and the presence of short ethyl groups, the amount of observed intermediates in DEE oxidation are

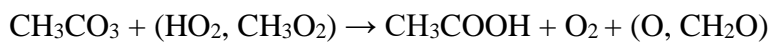
limited, unlike the case of dibutyl ether [12]. The major ones include formaldehyde, acetaldehyde, acetic acid (only at low temperatures), ethylene and methane (high temperature). The minor ones include ethane, propene and propane.

Reaction pathways of DEE oxidation in the JSR at 10 atm are investigated under lean conditions, at 510 K and 690 K both of which correspond to about 46% fuel conversion (Figure 5). At 510 K, fuel is consumed by OH radicals abstracting a hydrogen yielding the  $\alpha$ -radical  $\text{CH}_3\dot{\text{C}}\text{H}-\text{O}-\text{CH}_2\text{CH}_3$ , as shown in Figure 5. This radical adds to molecular oxygen forming the  $\text{RO}_2$  radical. The QOOH radical  $\text{CH}_3\dot{\text{C}}\text{H}-\text{O}-\text{CH}(\text{OOH})\text{CH}_3$ , results from isomerisation via a 6-membered ring transition state. This is the most energetically favorable QOOH to be formed. This radical then undergoes a second  $\text{O}_2$  addition, isomerization and OH elimination finally yielding the corresponding ketohydroperoxide. Its decomposition yields acetaldehyde observed below 500 K (Figs 2–4).

At 690 K, which corresponds to the NTC region, 97% of the fuel produces the  $\alpha$ -radical while about 3% of the flux yields the primary radical. The  $\alpha$ -radical  $\text{CH}_3\dot{\text{C}}\text{H}-\text{O}-\text{CH}_2\text{CH}_3$  adds to  $\text{O}_2$  (78% of the reaction flux) forming the  $\text{RO}_2$  then the QOOH radical  $\text{CH}_3\dot{\text{C}}\text{H}-\text{O}-\text{CH}(\text{OOH})\text{CH}_3$  by isomerization. This QOOH radical follows the pathway described above. On the other hand, 22% of the flux coming from the  $\alpha$ -radical leads to the formation of acetaldehyde via  $\beta$ -scission. One can see the peak value of acetaldehyde occurs around this temperature ( $\phi = 0.5$ , Fig. 2). At higher temperatures the branching ratio between these two reactions favors beta-scission. For example, at 800 K 87% of the flux yields acetaldehyde and ethyl radical.

Acetic acid, which is a major low-temperature intermediate is under-predicted by the model (about a factor of 2 at  $\phi = 0.5$ ). Major formation pathways of acetic acid at 550 K are:





and  $\text{CH}_3\text{CHO} + \text{OH} \rightleftharpoons \text{CH}_3\text{COOH} + \text{H}$ , to a minor extent.

Rate coefficients for the  $\text{CH}_3\text{CO}_3 + (\text{HO}_2, \text{CH}_3\text{O}_2)$  reactions were adopted from Atkinson et al. [26, 27]. The reaction  $\text{CH}_3\text{CO}_3 + \text{HO}_2$  leads to the formation of ozone, which, here, is replaced by  $\text{O} + \text{O}_2$ . Carboxylic acids have recently been observed in important quantities during low temperature oxidation of hydrocarbons [28, 29]. The pathways considered above under-estimate the important quantities of acetic acid in our study, this may be partly due to the uncertainties in the fate of the methylperoxy radicals ( $\text{CH}_3\text{O}_2$ ) as well as missing pathways. Methyl radicals are produced via decomposition of the acetyloxy radicals ( $\text{CH}_3\text{CO}_2$ ) which are abundant at low temperatures, being the product of the decomposition of the major ketohydroperoxide, as in Figure 5. At these low temperatures  $\text{CH}_3 + \text{O}_2 \rightleftharpoons \text{CH}_3\text{O}_2$  proceeds in the forward direction. While  $\text{CH}_3\text{O}_2$  radicals react via numerous pathways, according to the present model, 25% of its consumption forms acetic acid ( $\text{CH}_3\text{CO}_3 + \text{CH}_3\text{O}_2 \rightarrow \text{CH}_3\text{COOH} + \text{O}_2 + \text{CH}_2\text{O}$ ).

Ethane and small amounts of propane (15 ppm peak,  $\phi = 2$ ) are observed with peak values at 950 K, these are recombination products of the reactions  $\text{CH}_3 + \text{CH}_3 \rightleftharpoons \text{C}_2\text{H}_6 (+\text{M})$  and  $\text{CH}_3 + \text{C}_2\text{H}_5 (+\text{M}) \rightleftharpoons \text{C}_3\text{H}_8 (+\text{M})$ . A maximum of 10 ppm of propene was observed. It is formed by  $\text{HO}_2$  elimination from isopropylperoxide radical as well as oxidation of n- and isopropyl radicals. Kinetically, the major cyclic ether is expected to be 2,4-dimethyl-1,3-dioxetane, however this species has not been identified, most likely due to its relative instability. On the other hand traces of the 5-membered ring cyclic ether 2-methyl-1,3-dioxolane and ethoxyethene were identified.

### *1 atm experiments*

Figures 6–8 illustrate experimental results and model comparisons for the 1 atm experiments.

At atmospheric pressure, much less reactivity is observed at low temperature compared to 10 atm experiments. As a matter of fact, this small reactivity is experimentally observed only for  $\phi = 0.5$  and 1 mixtures and not for the rich one. The beginning of the high-temperature reactivity is also greater than the 10 atm cases; around 950 K for  $\phi = 0.5$  and 1000 K for the fuel-rich mixture. Intermediate species are similar to the 10 atm case except for ethanol observed as a result of the molecular reaction of DEE yielding ethanol and ethylene. This molecular reaction shows up only at 1 atm given that bimolecular reactions are favored at high pressures. One should note that the major production route for ethylene at 1 atm, remains the C–H scission of ethyl radicals. A reaction path diagram is shown for the  $\phi = 1$  mixture at 1050 K in Figure 9.

### *Comparison to DBE oxidation*

In a recent study from our group [12], the oxidation behavior of dibutyl ether (DBE) mixtures was investigated under same experimental conditions as in the present study. Figure 10 illustrates comparative plots on the evolution of fuel profile at 10 atm. According to this, for both fuels, reactivity begins around 470 K regardless of the equivalence ratio and profiles are similar for DEE showing, slightly more reactivity than DBE. In the NTC region and beyond, the two ethers show very different reactivity profiles. As opposed to the “double-NTC” behavior observed for the oxidation of DBE, DEE has a more “conventional” low-temperature reactivity profile approaching zero reactivity in a given temperature interval

depending on the equivalence ratio. DBE has a longer chain compared to DEE and forms more diverse radicals and molecules during its oxidation. At the lowest temperatures of interest, formation of ketohydroperoxides are favored and reactivity increases. In the case of DEE, decomposition of the major ketohydroperoxide leads to formation of acetaldehyde and methyl radicals while in the case of DBE, butanal and n-propyl radicals are formed, which complicates the intermediate temperature region chemistry. More detailed analyses on the behavior of DBE can be found in [12], while for DEE the cool flame chemistry under present experimental conditions is relatively “simpler” due to the short ethyl chain, although discrepancies and uncertainties exist, as presented above. These differences can be observed through the evolution of the intermediate species, which are more numerous in DBE oxidation in contrast to DEE oxidation. Dimethyl ether (DME) mole fraction profile from an earlier study of Dagaut et al. [30] is also plotted (Figure 10.b) in order to see a wider picture of how different this simplest ether is in terms of reactivity compared to DEE and DBE. DME exhibits low-temperature reactivity and NTC behavior as already known, however to a much smaller extent due to its small methyl chain. We should note that the experimental conditions are different in the former DME study; 2000 ppm initial fuel mole fraction and 1s of residence time, chosen in order to observe proper low-temperature reactivity. According to Figure 10.b, DME stands out with fuel conversion starting around 570 K, about 100 K higher than DEE and DBE, although the residence time was slightly higher in the DME study. On the other hand, they all show similar behavior as far as high temperature reactivity is concerned.

#### *Comparison to literature data*

The model presented in this study was tested against available literature data, i.e. flame speed, flame speciation and ignition delay times. Figure 11 illustrates ignition delay times of various DEE mixtures in argon or air reported by Yasunaga [6], and Werler [4] over different ranges of temperatures and pressures. The model agreement is quite good with the literature data,

especially with the shock tube data of Yasunaga et al (fig 11.a) and the high-pressure RCM data of Werler et al. (fig 11.b). The agreement with the 3 bar RCM data (fig 11.c) is good up to 770 K. Above 700 K, the model predicts longer ignition delays than reported [4]. The authors recently reported that their high-temperature data suffered from pre-ignition (data in gray, fig 11c). They performed new measurements in this region and the new ignition delays are considerably longer [31], but this study is not yet published.

Figure 12 shows laminar flame speeds of DEE/air mixtures as a function of equivalence ratio [1] and as a function of pressure for an equivalence ratio of 1.4 [2]. The model is in good agreement with the data in Fig. 12(a), the discrepancy for the peak value at 398 K is 5%. On the other hand, there is considerable under-prediction compared to the data in Fig. 12(b) by around 20%. This discrepancy, also occurring with authors' model, was explained by uncertainties in the base mechanism or uncertainties in the experiment. In the same paper, authors also present speciation data from a fuel-rich flat flame. The predictions of the present model are in reasonable agreement with the data and these are given in the supplementary material.

#### **4. Conclusions**

The oxidation of DEE was investigated experimentally in a jet-stirred reactor at same conditions as in our DBE study [12]. Similarly to dimethyl and dibutyl ethers, DEE shows early reactivity, around 470 K under the investigated conditions. At 10 atm, DEE showed strong cool flame and NTC behavior, at the end of which reactivity almost went back to zero. This was not the case in DBE oxidation where multiple reactivity regions were observed. Low-temperature reactivity is observed at 1 atm experiments as well, for the fuel-lean and stoichiometric mixtures, always weaker than 10 atm cases supported by the formation of formaldehyde, acetaldehyde, and acetic acid. Due to its short chain, DEE oxidation produced

a limited number of stable molecules including formaldehyde, high amounts of acetaldehyde and acetic acid in the cool flame region at 10 atm. Note that no acetic acid was detected in 1 atm experiments for  $\varphi = 2$  mixture and no carboxylic acids were detected in the previous DBE study at 1 atm either (only some formic acid was detected with a peak of 40 ppm at  $\varphi = 0.5$  in DBE oxidation). A reaction sub-mechanism was developed mainly based on calculations in literature and our previous study [12]. This mechanism was tested against the present and literature data, the overall agreement is found to be good. In the JSR comparisons, discrepancies mostly lie on the uncertainties in the low-temperature chemistry of small species as presented in the pathway analysis.

## 5. Acknowledgements

Authors gratefully acknowledge funding received from Labex Caprysses (convention ANR-11-LABX-0006-01).

## References

- [1] F. Gillespie, W.K. Metcalfe, P. Dirrenberger, O. Herbinet, P.-A. Glaude, F. Battin-Leclerc, H.J. Curran, Measurements of flat-flame velocities of diethyl ether in air, *Energy* 43 (2012) 140-145.
- [2] L.-S. Tran, J. Pieper, H.-H. Carstensen, H. Zhao, I. Graf, Y. Ju, F. Qi, K. Kohse-Höinghaus, Experimental and kinetic modeling study of diethyl ether flames, *Proceedings of the Combustion Institute* 36 (2017) 1165-1173.
- [3] L.-S. Tran, J. Pieper, M. Zeng, Y. Li, X. Zhang, W. Li, I. Graf, F. Qi, K. Kohse-Höinghaus, Influence of the biofuel isomers diethyl ether and n-butanol on flame structure and pollutant formation in premixed n-butane flames, *Combustion and Flame* 175 (2017) 47-59.

- [4] M. Werler, L.R. Cancino, R. Schiessl, U. Maas, C. Schulz, M. Fikri, Ignition delay times of diethyl ether measured in a high-pressure shock tube and a rapid compression machine, *Proceedings of the Combustion Institute* 35 (2015) 259-266.
- [5] N. Vin, O. Herbinet, F. Battin-Leclerc, Diethyl ether pyrolysis study in a jet-stirred reactor, *Journal of Analytical and Applied Pyrolysis* 121 (2016) 173-176.
- [6] K. Yasunaga, F. Gillespie, J.M. Simmie, H.J. Curran, Y. Kuraguchi, H. Hoshikawa, M. Yamane, Y. Hidaka, A Multiple Shock Tube and Chemical Kinetic Modeling Study of Diethyl Ether Pyrolysis and Oxidation, *The Journal of Physical Chemistry A* 114 (2010) 9098-9109.
- [7] W.G. Agnew, J.T. Agnew, Composition profiles of the diethyl ether-air two-stage reaction stabilized in a flat-flame burner, *Symposium (International) on Combustion* 10 (1965) 123-138.
- [8] N. Zhang, Y. Di, Z. Huang, B. Zheng, Z. Zhang, Experimental Study on Combustion Characteristics of N<sub>2</sub>-Diluted Diethyl Ether–Air Mixtures, *Energy & Fuels* 23 (2009) 5798-5805.
- [9] Y. Di, Z. Huang, N. Zhang, B. Zheng, X. Wu, Z. Zhang, Measurement of Laminar Burning Velocities and Markstein Lengths for Diethyl Ether–Air Mixtures at Different Initial Pressure and Temperature, *Energy & Fuels* 23 (2009) 2490-2497.
- [10] Y. Sakai, H. Ando, H.K. Chakravarty, H. Pitsch, R.X. Fernandes, A computational study on the kinetics of unimolecular reactions of ethoxyethylperoxy radicals employing CTST and VTST, *Proceedings of the Combustion Institute* 35 (2015) 161-169.
- [11] Y. Sakai, J. Herzler, M. Werler, C. Schulz, M. Fikri, A quantum chemical and kinetics modeling study on the autoignition mechanism of diethyl ether, *Proceedings of the Combustion Institute* 36 (2017) 195-202.
- [12] S. Thion, C. Togbé, Z. Serinyel, G. Dayma, P. Dagaut, A chemical kinetic study of the oxidation of dibutyl-ether in a jet-stirred reactor, *Combustion and Flame* 185 (2017) 4-15.
- [13] R. Sivaramakrishnan, M.C. Su, J.V. Michael, S.J. Klippenstein, L.B. Harding, B. Ruscic, Rate Constants for the Thermal Decomposition of Ethanol and Its Bimolecular Reactions with OH and D: Reflected Shock Tube and Theoretical Studies, *The Journal of Physical Chemistry A* 114 (2010) 9425-9439.
- [14] C.-W. Zhou, J.M. Simmie, H.J. Curran, An ab initio/Rice-Ramsperger-Kassel-Marcus study of the hydrogen-abstraction reactions of methyl ethers, H<sub>3</sub>COCH<sub>3</sub>-x(CH<sub>3</sub>)<sub>x</sub>, x = 0-2, by [radical dot]OH; mechanism and kinetics, *Physical Chemistry Chemical Physics* 12 (2010) 7221-7233.

- [15] T. Ogura, A. Miyoshi, M. Koshi, Rate coefficients of H-atom abstraction from ethers and isomerization of alkoxyalkylperoxy radicals, *Physical Chemistry Chemical Physics* 9 (2007) 5133-5142.
- [16] J. Mendes, C.-W. Zhou, H.J. Curran, Rate Constant Calculations of H-Atom Abstraction Reactions from Ethers by HO<sub>2</sub> Radicals, *The Journal of Physical Chemistry A* 118 (2014) 1300-1308.
- [17] Z.F. Xu, J. Park, M.C. Lin, Thermal decomposition of ethanol. III. A computational study of the kinetics and mechanism for the CH<sub>3</sub>+C<sub>2</sub>H<sub>5</sub>OH reaction, *The Journal of Chemical Physics* 120 (2004) 6593-6599.
- [18] C.F. Goldsmith, W.H. Green, S.J. Klippenstein, Role of O<sub>2</sub> + QOOH in Low-Temperature Ignition of Propane. 1. Temperature and Pressure Dependent Rate Coefficients, *The Journal of Physical Chemistry A* 116 (2012) 3325-3346.
- [19] S.M. Villano, L.K. Huynh, H.-H. Carstensen, A.M. Dean, High-Pressure Rate Rules for Alkyl + O<sub>2</sub> Reactions. 1. The Dissociation, Concerted Elimination, and Isomerization Channels of the Alkyl Peroxy Radical, *The Journal of Physical Chemistry A* 115 (2011) 13425-13442.
- [20] S.M. Villano, L.K. Huynh, H.-H. Carstensen, A.M. Dean, High-Pressure Rate Rules for Alkyl + O<sub>2</sub> Reactions. 2. The Isomerization, Cyclic Ether Formation, and β-Scission Reactions of Hydroperoxy Alkyl Radicals, *The Journal of Physical Chemistry A* 116 (2012) 5068-5089.
- [21] C. Muller, V. Michel, G. Scacchi, G.M. Côme, Thergas - A computer program for the evaluation of thermochemical data of molecules and free radicals in the gas phase, *Journal de chimie physique et de physico-chimie biologique* 92 (1995) 1154-1178.
- [22] S.W. Benson, *Thermochemical Kinetics*, Wiley, New York, 1976.
- [23] P. Glarborg, R.J. Kee, J.F. Grcar, J.A. Miller, PSR: A Fortran Program for Modeling Well-Stirred Reactors, Report No. SAND86-8209, Sandia National Laboratories, Albuquerque, NM, 1986.
- [24] A.E. Lutz, R.J. Kee, M.J. A., SENKIN: A Fortran program for predicting homogeneous gas phase chemical kinetics with sensitivity analysis, Report No. SAND-87-8248, Livermore, CA, 1988.
- [25] J.F. Kee, J.F. Grcar, J.A. Miller, M.D. Smooke, E. Meeks, PREMIX, Report No. SAND85-8240, Livermore, CA, 1985.
- [26] R. Atkinson, D.L. Baulch, R.A. Cox, J.N. Crowley, R.F. Hampson, R.G. Hynes, M.E. Jenkin, M.J. Rossi, J. Troe, I. Subcommittee, Evaluated kinetic and photochemical data for

atmospheric chemistry: Volume II &ndash; gas phase reactions of organic species, *Atmos. Chem. Phys.* 6 (2006) 3625-4055.

[27] R. Atkinson, D.L. Baulch, R.A. Cox, R.F.H. Jr., J.A. Kerr, J. Troe, Evaluated Kinetic and Photochemical Data for Atmospheric Chemistry: Supplement IV. IUPAC Subcommittee on Gas Kinetic Data Evaluation for Atmospheric Chemistry, *Journal of Physical and Chemical Reference Data* 21 (1992) 1125-1568.

[28] O. Herbinet, B. Husson, Z. Serinyel, M. Cord, V. Warth, R. Fournet, P.-A. Glaude, B. Sirjean, F. Battin-Leclerc, Z. Wang, M. Xie, Z. Cheng, F. Qi, Experimental and modeling investigation of the low-temperature oxidation of n-heptane, *Combustion and Flame* 159 (2012) 3455-3471.

[29] J. Bugler, A. Rodriguez, O. Herbinet, F. Battin-Leclerc, C. Togbé, G. Dayma, P. Dagaut, H.J. Curran, An experimental and modelling study of n-pentane oxidation in two jet-stirred reactors: The importance of pressure-dependent kinetics and new reaction pathways, *Proceedings of the Combustion Institute* 36 (2017) 441-448.

[30] P. Dagaut, C. Daly, J.M. Simmie, M. Cathonnet, The oxidation and ignition of dimethylether from low to high temperature (500–1600 K): Experiments and kinetic modeling, *Symposium (International) on Combustion* 27 (1998) 361-369.

[31] M. Fikri, Y. Sakai, J. Herzler, C. Schulz, Experimental and numerical study of the ignition delay times of primary reference fuels containing diethyl ether, 26th ICDERS, Boston, MA, 2017.

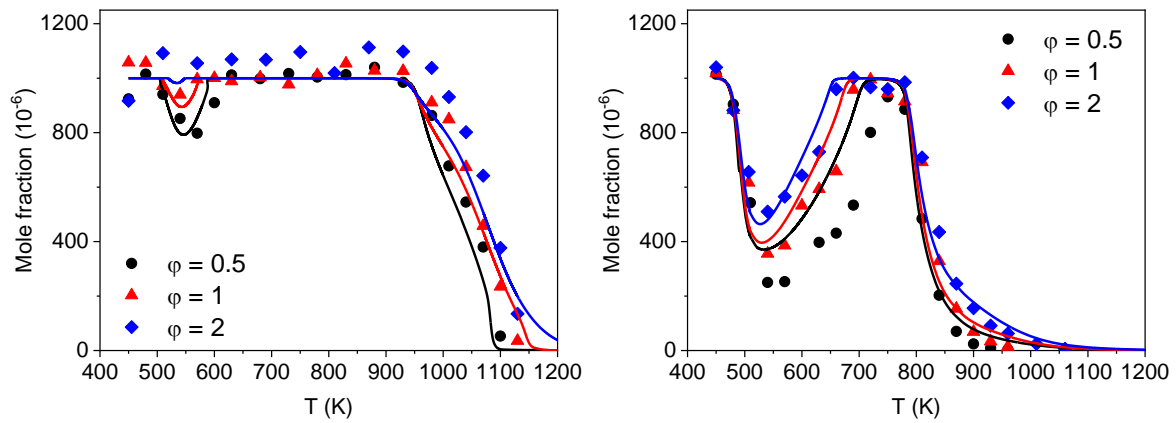


**Figure 1.** DEE mole fraction evolution as a function of temperature, 1 atm (left), 10 atm (right), lines represent simulations.

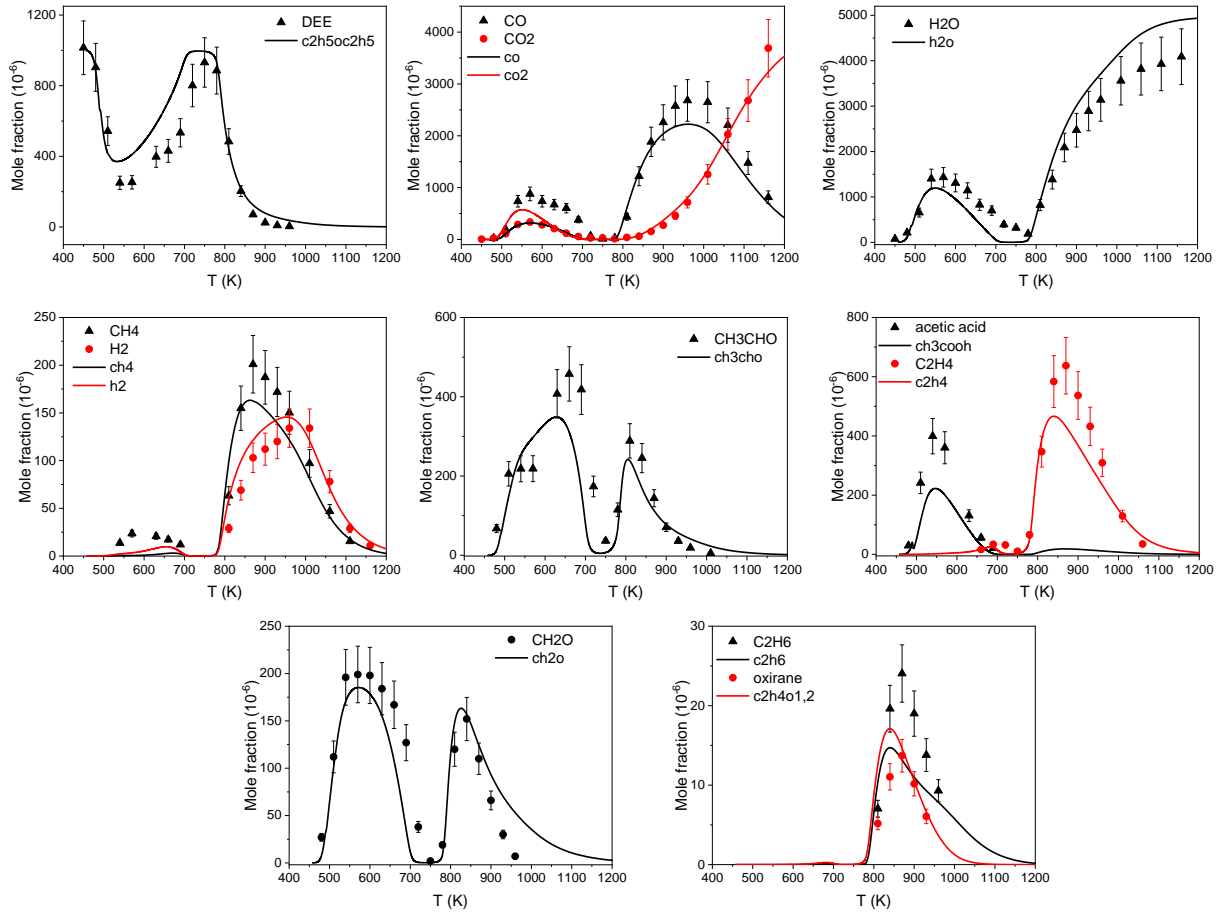


**Figure 2.** Mole fraction profiles for the  $\phi = 0.5$  experiment at 10 atm, initial mole fraction of DEE: 1000 ppm,  $\tau = 0.7$ s.

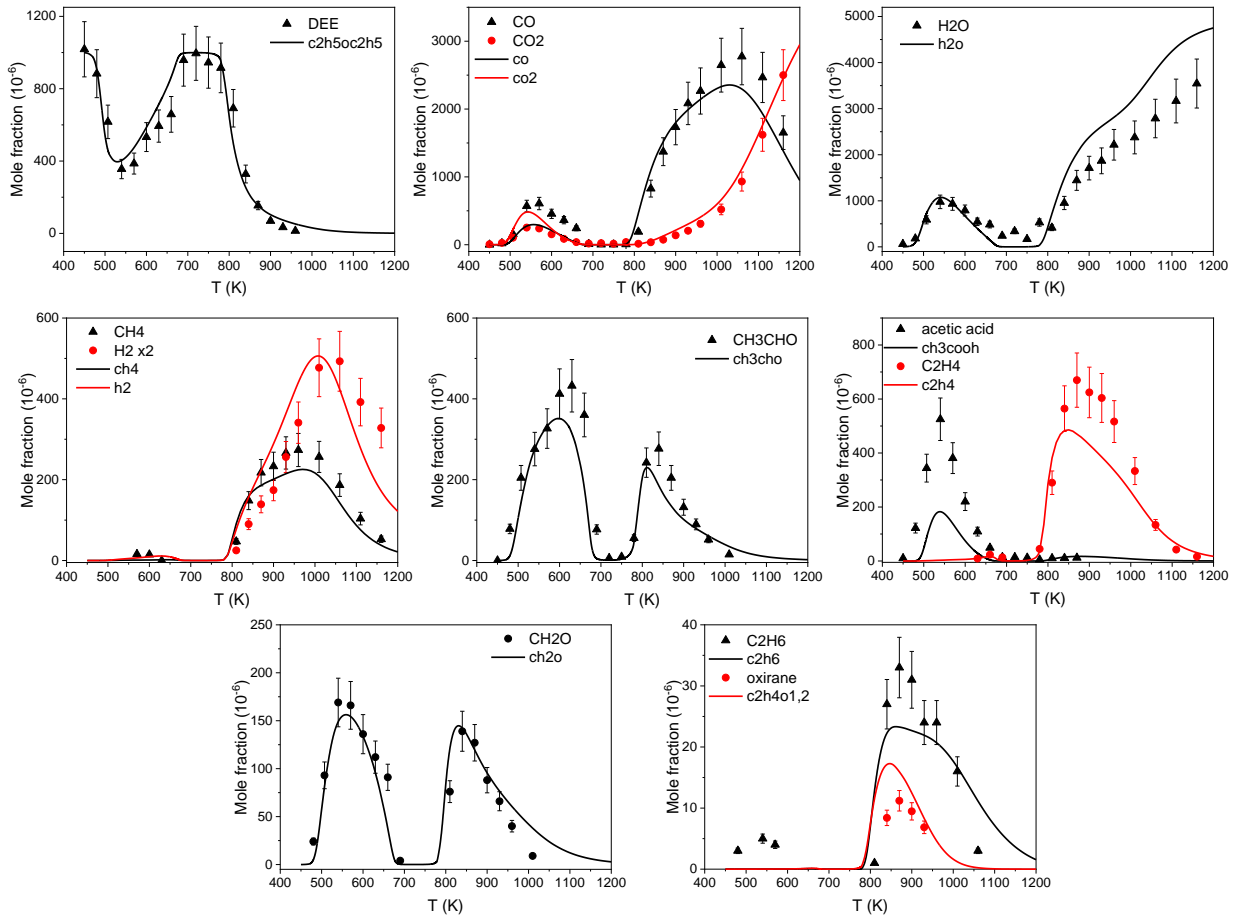


**Figure 3.** Mole fraction profiles for the  $\phi = 1$  experiment at 10 atm, initial mole fraction of DEE: 1000 ppm,  $\tau = 0.7s$ .

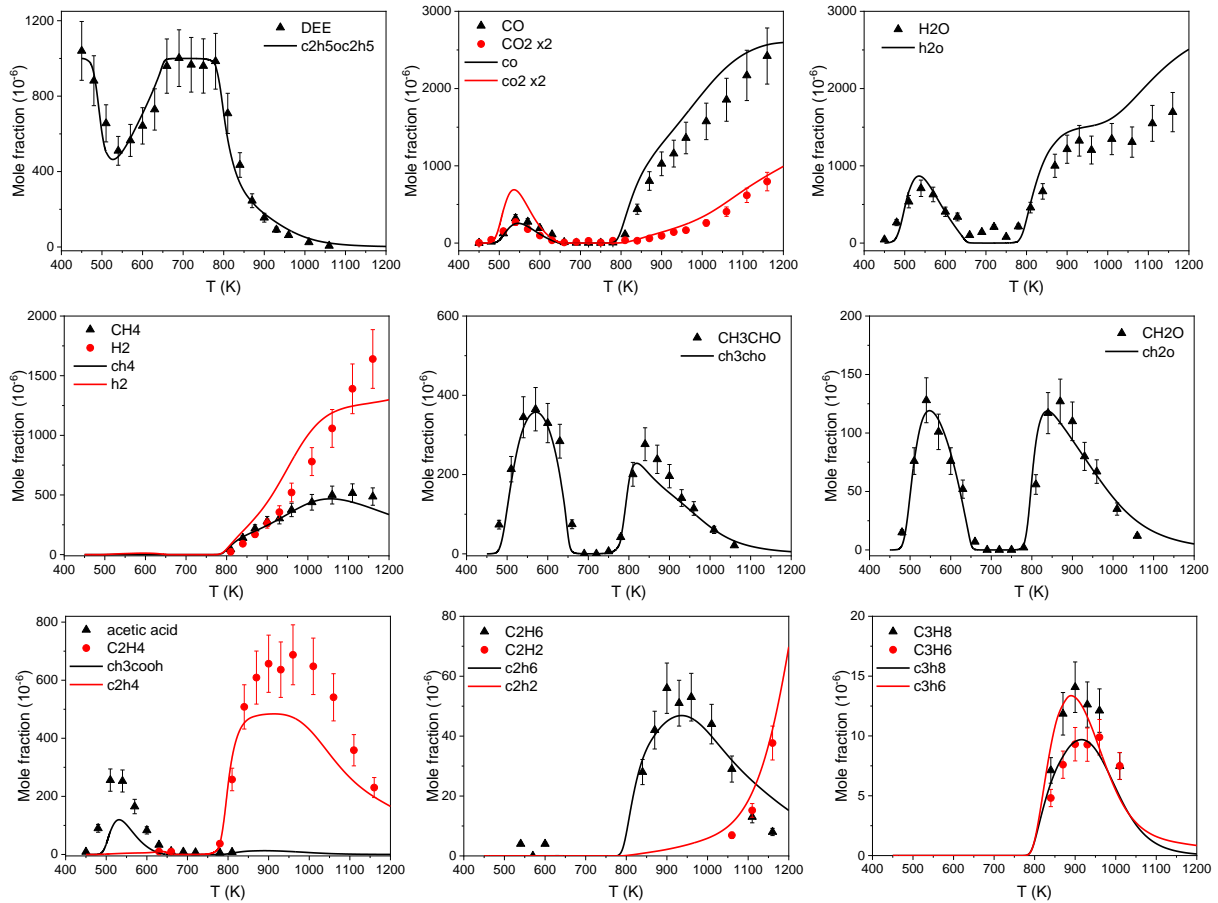


**Figure 4.** Mole fraction profiles for the  $\phi = 2$  experiment at 10 atm, initial mole fraction of DEE: 1000 ppm,  $\tau = 0.7$ s.

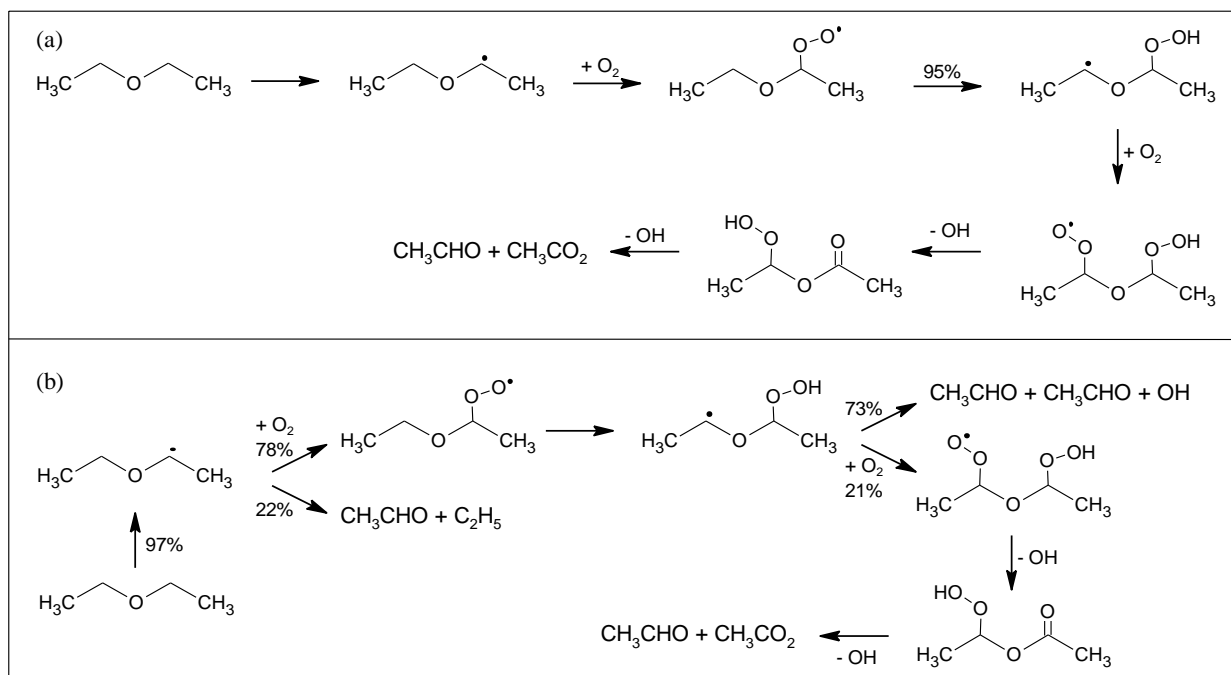


**Figure 5.** Reaction pathways at (a) 510 K and (b) 690 K (10 atm,  $\phi = 0.5$ )

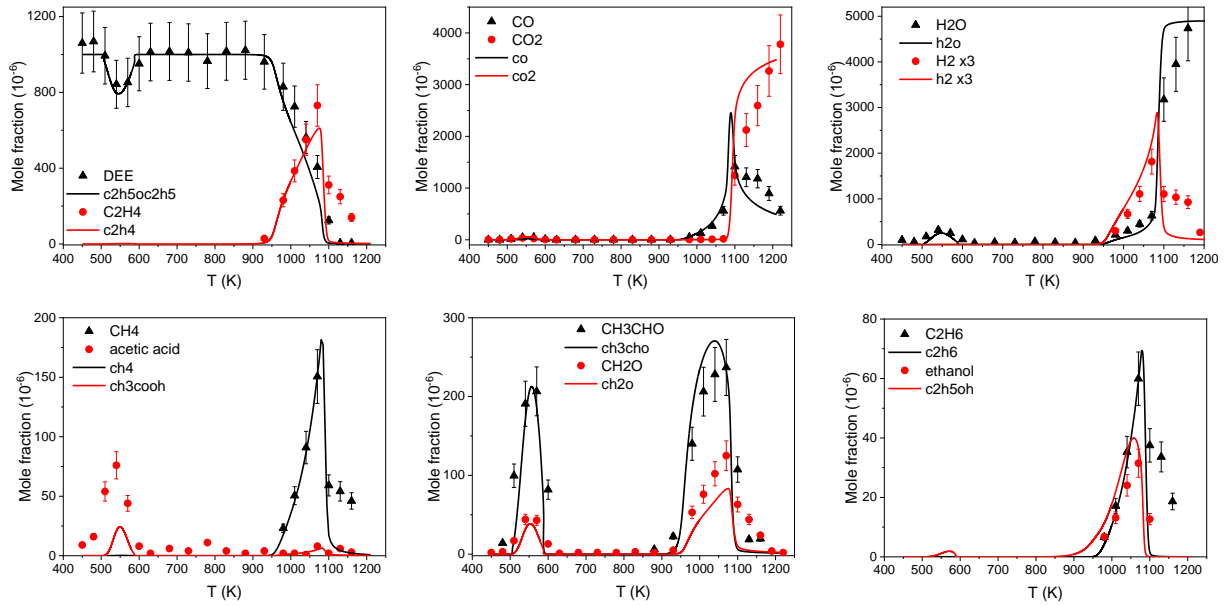


**Figure 6.** Mole fraction profiles for the  $\phi = 0.5$  experiment at 1 atm, initial mole fraction of DEE: 1000 ppm,  $\tau = 0.07$ s.

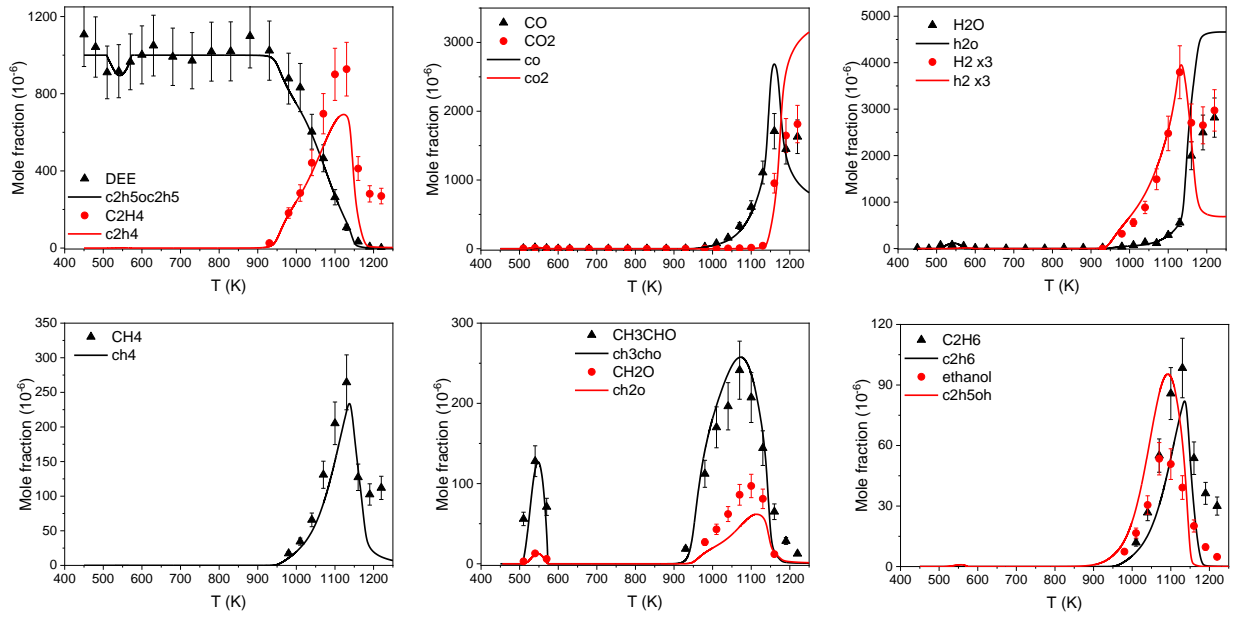


**Figure 7.** Mole fraction profiles for the  $\phi = 1$  experiment at 1 atm, initial mole fraction of DEE: 1000 ppm,  $\tau = 0.07s$ .

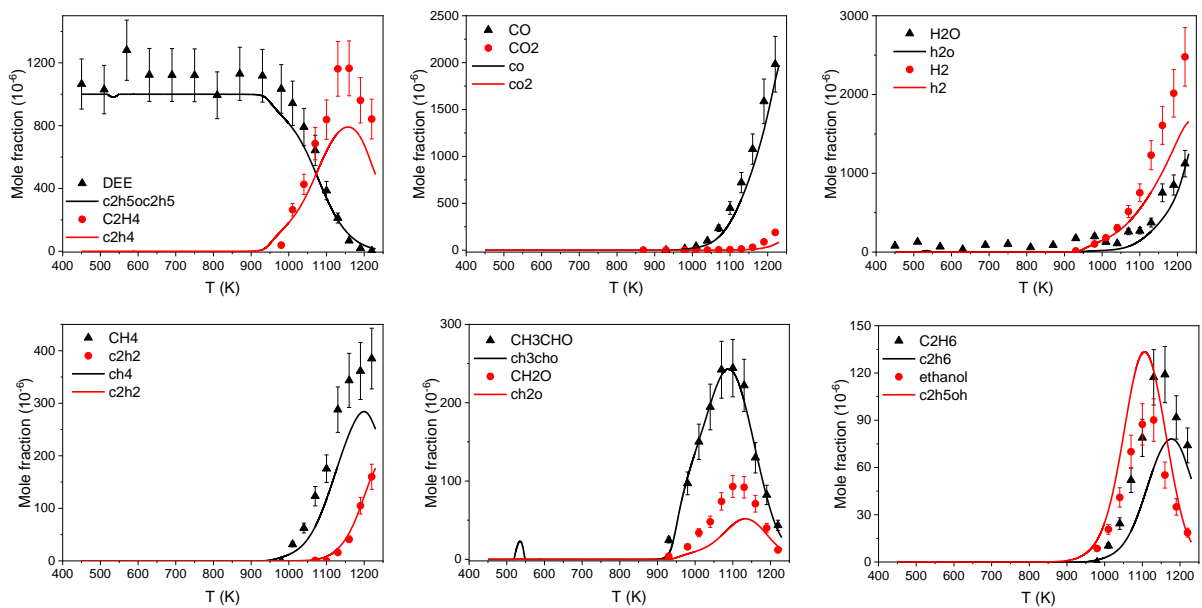


**Figure 8.** Mole fraction profiles for the  $\phi = 2$  experiment at 1 atm, initial mole fraction of

DEE: 1000 ppm,  $\tau = 0.07s$ .

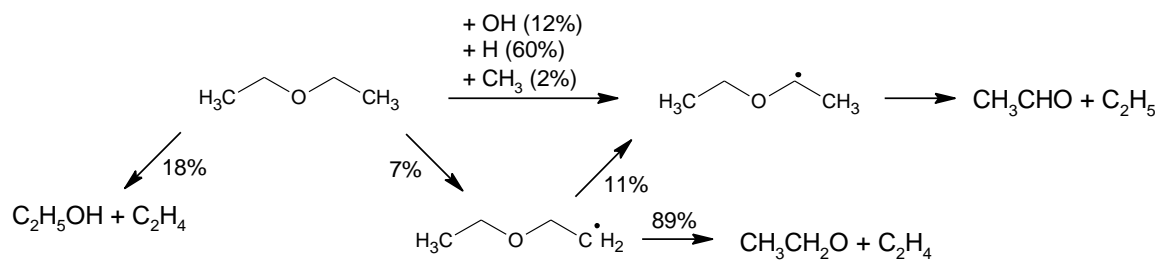


**Figure 9.** Fuel decomposition pathways at 1050 K (1 atm,  $\phi = 1$ )

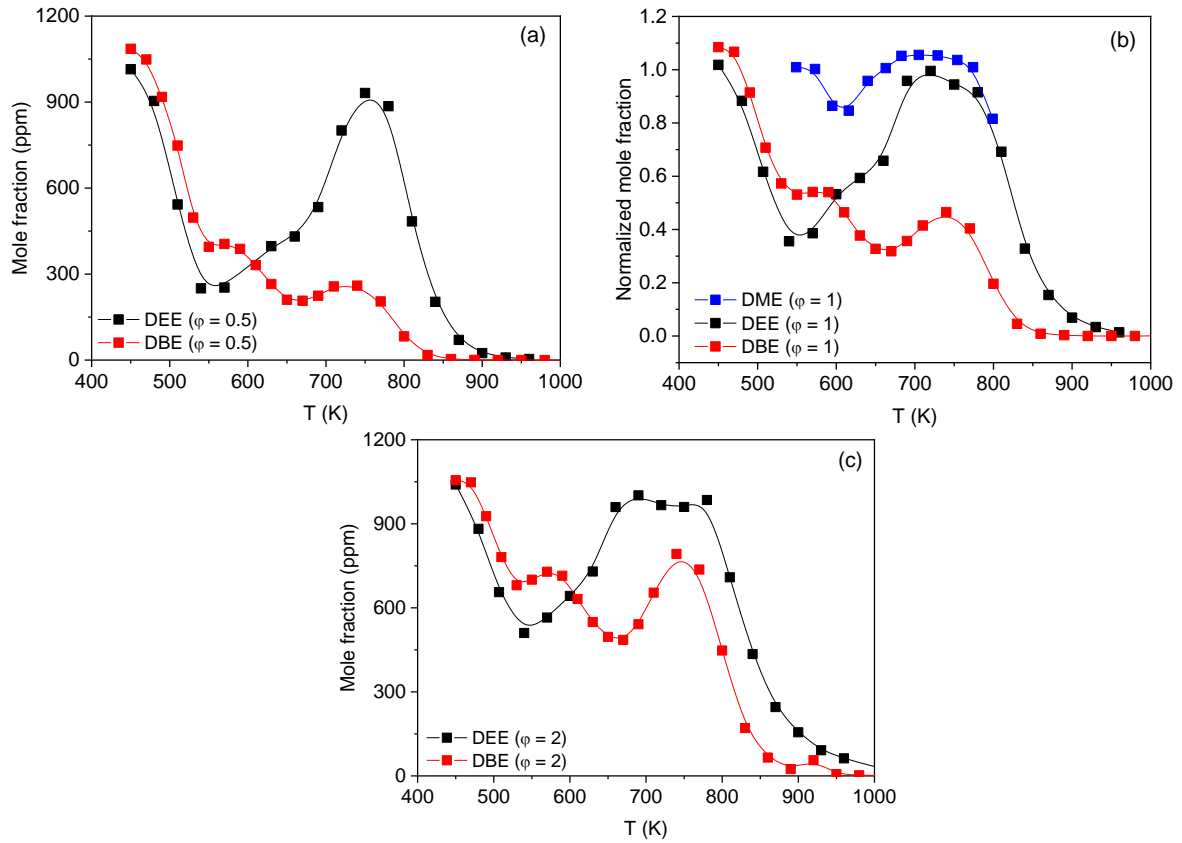


**Figure 10.** Evolution of fuel mole fraction profiles of DEE (this study), DBE [12] and DME [30] at 10 atm (lines are added to guide the eye). Experimental conditions for DBE and DEE: 10 atm, 0.1% fuel, residence time of 0.7s. Experimental conditions for DME: 10 atm, 0.2% DME, residence time of 1s.

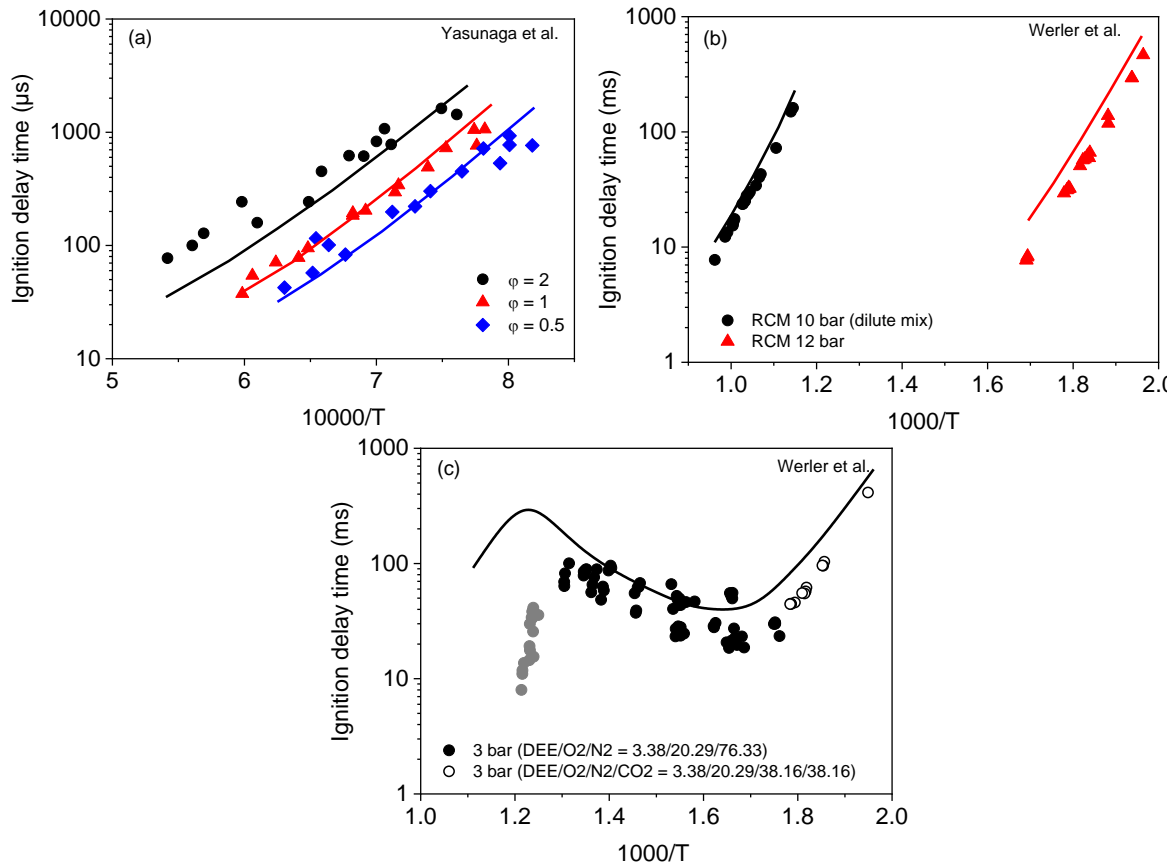


**Figure 11.** Shock tube and rapid compression machine ignition delay times of (a) 1% DEE in argon,  $p = 1$  atm, shock tube data [6] (b) 0.698% DEE in argon,  $\phi = 1$ ,  $p = 10$ – $12$  bar, ST data [4] (c) DEE in air,  $\phi = 1$ , RCM data [4] (in simulations, reported experimental pressures were used, RCM data were calculated as constant volume system).

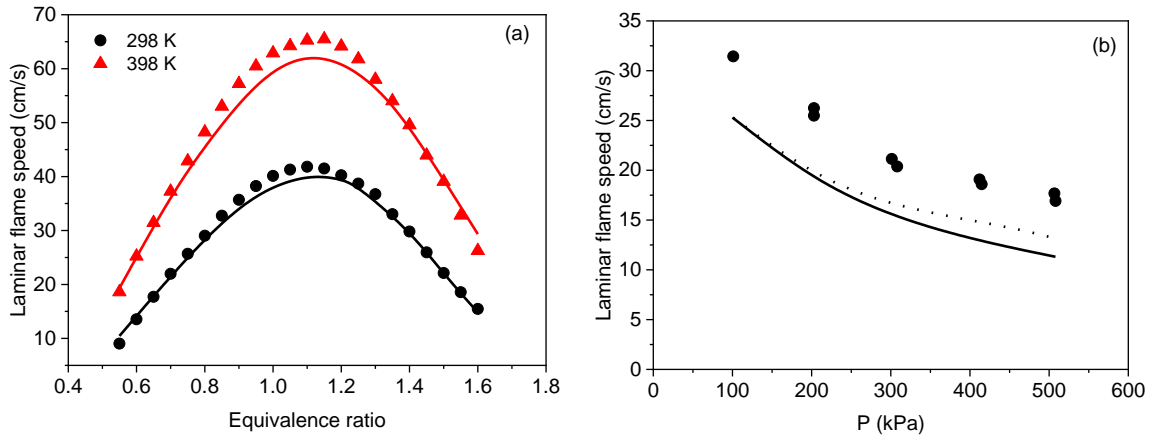


**Figure 12.** Laminar flame speed of DEE/air mixtures (a) as a function of equivalence ratio at 1 atm,  $T_u = 298$  and 398 K [1] (b) as a function of pressure for  $\phi = 1.4$ ,  $T_u = 298$  K [2], dotted line represents simulations with Tran et al [2] as presented in their paper, solid line represents simulations with the present mechanism.